A Spectroelectrochemical Investigation of the Reduction of the Water-Soluble MnTSPP: SERS Spectra of Mn^{II}TSPP

Shi-Ping Chen, David Ejeh, Dianne Levermore, Heidi Griffith, Yemi Bullen, Charles M. Hosten,* and Peter Hambright

Department of Chemistry, Howard University, Washington, D.C. 20059

Received: February 27, 1998; In Final Form: September 9, 1998

Electrochemical and surface spectroscopic techniques are used to investigate the reductive electrochemistry of the water-soluble manganese tetrasulfonatophenyl porphyrin. The electrocehmistry of MnTSPP at a Ag, Au, and Pt electrode and the normal Raman and surface-enhanced Raman scattering spectra of the two redox forms of MnTSPP were studied. Voltammetric studies indicate two reductive peaks at −0.45 and −0.85 V on an Ag electrode. Potential-dependent shifts in the 466 nm UV/vis absorbance band to 432 nm at −0.5 V on a gold minigrid electrode indicate that reduction of the porphyrin central metal from Mn^{III} to Mn^{II} occurs at this potential. A 32 cm^{-1} downshift in the ν_4 vibration from 1368 to 1336 cm^{-1} at −0.5 V is further evidence for the reduction of the metal from the Mn^{III} to the Mn^{II} state. The reduction of the porphyrin macrocyclic ring to the radical anion is also observed at −0.8 V. The core-sensitive modes of aquo Mn^{III}-TSPP are in excellent agreement with that of a 6-coordinate species. Upon reduction to the Mn^{II}TSPP, the core size marker frequencies shift to those of a 5-coordinate species. Finally, Raman band frequencies for the solution and SERS spectra are systematically assigned, and normal Raman and surface-enhanced Raman spectra are presented for Mn^{III}TSPP and its reduced Mn^{II}TSPP.

Introduction

The fundamental engine driving porphyrin and heme protein research continues to be the development of a correlation between porphyrin structural and electronic factors and the wide range of catalytic properties exhibited by heme proteins.[1−3]

Manganese porphyrins display a wide variety of interesting physical and chemical properties, and the addition of functional groups to increase their solubility in water makes them suitable model compounds for research related to biological phenomena.[4] Particular interest lies in mimicking the role of the Mn complex in photosystem II, in which a manganese complex catalyzes the reaction between a quinone and water leading to the hydroquinone and molecular oxygen.[5] The manganese complex involved in photosystem II undergoes charge accumulation, which requires that the metal possess a series of available redox states. Mn porphyrins have been shown to fulfill this requirement.[6]

High valent manganese intermediates were postulated by a number of groups,[7−10] and high valent manganese−oxo porphyrin complexes were proposed as the catalytically active species in efficient biomimetic systems for hydrocarbon oxidations.[11,12]

Surface-enhanced Raman scattering spectroscopy (SERS) has found application at probing molecules adsorbed onto electrode surface and providing information on the molecular structure, orientation and conformation of adsorbates.[13−15] The technique has found application as an in situ mechanistic probe of heterogeneous catalytic systems at high gas pressure, providing molecular level interfacial information.[16]

SERS has been successfully applied to the characterization of molecular species formed during electrochemical reduction processes.[17−19] Rubim and co-workers[20] used the molecular information provided by SERS to characterize the electrochemical intermediates formed during the reduction of $(M(bipy)_3)^{2+}$. The specificity of the information obtained by SERS allowed for the differentiation between the metal reduction and the reduction of the bipyridyl system to form the bipyridyl radical anion. Spiro et al.[21] also monitored the metal-centered reduction of Fe^{III}PPDME on a silver electrode using SERS spectroscopy. The adsorbed Fe^{III} and Fe^{II} species were characterized on the electrode surface, and the non-Nernstien behavior of the transition was followed using SERS spectroscopy. The transition from high-spin Fe^{III} heme to high-spin Fe^{II} heme in iron protoporphyrin dissolved in basic solution has been followed by SERS. A number of SERS studies of porphyrins[22−30] adsorbed onto silver sols have been performed with either the aggregation state of the adsorbed porphyrin or the incorporation of Ag into the free base porphyrins on adsorption onto the silver metal surface as their primary concerns.

Time-resolved SERS in the microsecond time domain was successfully applied to the characterization and lifetime determination of transient electrochemically generated species on a silver electrode surface.[31,32]

In this study, surface-enhanced Raman spectroscopy, along with cyclic voltammetry, differential pulse voltammetry, and potential-dependent UV−vis spectroscopy, was utilized to monitor the reduction of Mn^{III}TSPP on an electrode surface. The ability of SERS to distinguish reduction products at the molecular level is used to characterize the Mn^{III}/Mn^{II} transition. The results were analyzed in terms of the coordination state of the Mn^{III} and the electrogenerated Mn^{II} species along with the orientation and aggregation state of the adsorbed porphyrin on the electrode surface.

Experimental Section

Manganese TSPP was synthesized and purified using standard literature procedures, and porphyrin composition and purity were confirmed by NMR and IR spectroscopy.

* To whom correspondence should be addressed. Telephone (202) 806-6829.

10.1021/jp981350z CCC: $15.00
Published on Web 10/16/1998

SERS spectra were acquired from the porphyrin molecule adsorbed on an electrochemically roughened electrode. Dilute solutions of the porphyrin, approximately 10^{-5} M with 0.1 M KCl as supporting electrolyte, were used for the SERS experiments. The sample cell for SERS consisted of a 99.999% pure silver working electrode (Aldrich Chemicals), a platinum counter electrode, and a saturated calomel electrode (Bioanalytical Systems), served as the reference. Prior to obtaining SERS spectra, the silver electrode surface was first mechanically polished with 0.3 μm and then 0.05 μm alumina (Buehler Inc.). The electrode surface was then washed and sonicated in distilled water. The oxidation reduction cycle (ORC) pretreatment was performed in situ using two 2 s pulses from 0.0 to −0.3 V and then returning to 0.0 V. To eliminate the contribution from solution species in the SERS spectra, the SERS cell was physically washed with an electrolyte blank at the completion of the ORC. The resulting SERS spectra were obtained from surface species devoid of any solution contributions.

Normal solution Raman and SERS scattered light were collected at 90° by a Nikon f/1.2 camera lens and collimated using a f/4 50 mm lens (Melles Griot). The radiation was collimated onto the slit of a 0.5 m spectrograph (Spex Instruments model 500M) containing interchangeable 1200 and 1800 groove/mm holographic gratings. A 50 mm holographic filter (Kaiser Optical) was placed between the entrance slit and the collimating lens to assist in stray light reduction. The excitation source was a Spectra Physics model 164 argon ion laser providing excitation at 488 and 514 nm. The detection system was an EG+G air-cooled 1530-A/UV 1024S CCD detector controlled by a Gateway 66 MHz 486 computer. The electrochemical system for the SERS experiments consisted of a PAR model 175 universal programmer and a PAR model 362 scanning potentiostat. The solution Raman and SERS spectra were calibrated using the known frequencies of indene and fenchone, and the spectroscopic system had a resolution of 2 cm^{-1}. The band assignments and numbering system followed those given for the modes of nickel tetraphenyl porphyrin and were located by frequency patterns. Because all SERS bands show similar polarization characteristics, they could not be assigned based on their polarization properties.

For the electrochemical studies, 10^{-3} M solutions of MnTSPP were prepared by dissolving the porphyrin in deionized distilled water. Potassium chloride (0.1 M, Fisher Analytical Grade) served as the supporting electrolyte, and the resulting solution was degassed using prepurified grade nitrogen (Air Products and Chemicals Inc.). Prior to performing the electrochemical experiments, the electrode was polished and sonicated using the procedure described in the previous section.

Cyclic voltammetry (CV) and differential pulse voltammetry (DPV) were performed using a BAS 100B electrochemical workstation that was interfaced to a 133 MHz Gateway computer. CV was performed using a starting potential of 0.0 V and a switching potential of −1.0 V with scan rates varying from 10 to 1500 mV/s. A conventional three-electrode system was used, consisting of a platinum counter electrode, saturated calomel electrode (SCE), and either a silver, platinum, or gold working electrode, with a diameter of approximately 1.6 mm. The electrodes were provided by BioAnalytical Systems, and all potentials are referenced to the SCE. All measurements were performed at room temperature.

A thin-layer spectroelectrochemical cell was fabricated for the potential-dependent UV−vis absorption experiments. A gold minigrid with 60% optical transparency was sandwiched between two optically transparent glass slides and served as the working electrode. This working electrode had an optical path length of less than 1 mm and was placed in a glass reservoir containing a dilute, degassed solution of the porphyrin and supporting electrolyte. Transport of the porphyrin solution into the working electrode was by capillary action. A platinum counter electrode and a saturated calomel reference electrode were in contact with the porphyrin solution. The potential of the system was altered using a Bioanalytical Systems CV-27 voltammograph, and absorption spectra were recorded by an HP 8453 UV−vis diode array spectrophotometer. The sample cavity of the spectrometer was constantly purged with nitrogen gas during the acquisition of absorbance spectra.

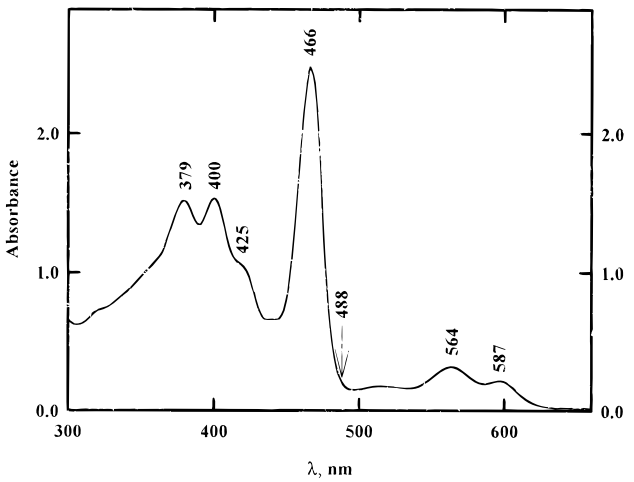

Figure 1. UV−vis absorption spectrum of MnTSPP indicating the relationship between the Soret band and 488 nm laser excitation.

Chemical reduction of the MnTSPP was also performed by first bubbling a dilute solution of the porphyrin with nitrogen gas, followed by the anaerobic addition of a few milligrams of sodium dithionite. The UV−vis absorbance spectrum of this chemically reduced Mn TSPP in a conventional 1 mm sample cell was then obtained using an HP UV−vis 8453 diode array spectrometer.

Results

Figure 1 shows the UV−vis absorption spectrum of a dilute 10^{-5} M aqueous solution of MnTSPP. In the spectral region displayed, 300−650 nm, the most intense absorption band is observed at 466 nm. A pair of bands at 400 and 379 nm is also observed along with a shoulder at 425 nm. Less intense bands are observed at 564 and 587 nm. Because of their unusual electronic structure, Mn^{III} porphyrins exhibit atypical electronic absorption spectra. The absorption spectrum shown in Figure 1 for MnTSPP closely resembles the absorption spectrum of tetraphenylporphinato manganese(III) chloride reported by Sarkar et al.[33] The absorption bands show similar relative band intensities, and the wavelength differences are under 6 nm. The intense band around 466 nm has been assigned to a charge-transfer transition by Asher and co-workers[34] while Gouterman and co-workers[35] have ascribed it to a charge transfer mixed with π to π^* character.

Laser excitation, for the SERS experiments, was performed at 488 nm, which is 22 nm from the intense band at 466 nm. The arrow in Figure 1 indicates the position of the excitation source relative to the porphyrin absorption band. As a result, the presented SERS spectra are not resonance enhanced.

A Beer's law plot of absorbance as a function of solution concentration over the concentration range 2×10^{-5} to $5 \times$

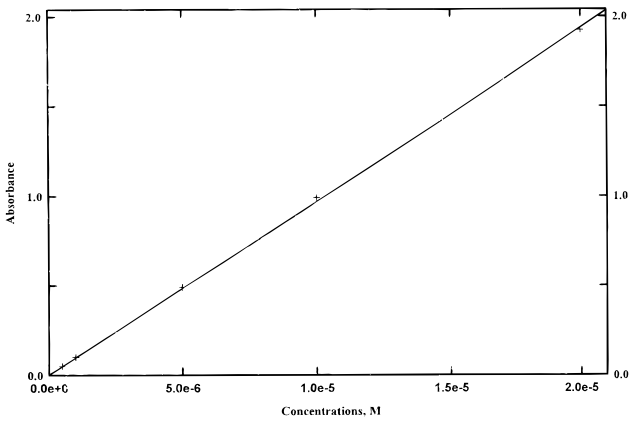

Figure 2. Plot of absorbance vs concentration for Mn^{III}TSPP dissolved in aqueous solution.

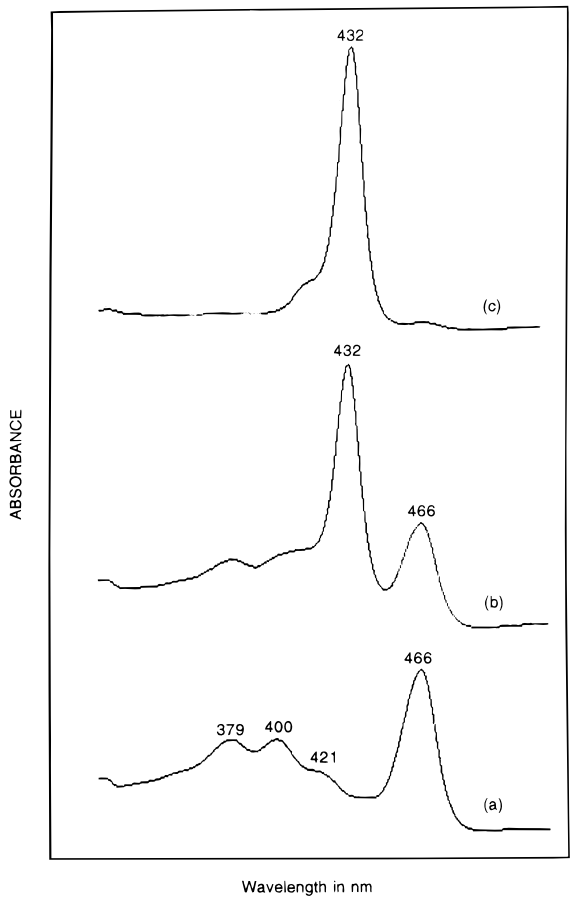

Figure 3. Potential-dependent UV−vis spectra of 10^{-4} M MnTSPP with a gold minigrid working electrode, a SCE, and a Pt counter electrode.

10^{-7} M for MnTSPP in aqueous solution is shown in Figure 2 for the 466 nm absorption band.

Potential-dependent UV−vis absorption spectroscopy was performed on dilute solutions of MnTSPP using a gold minigrid as the working electrode. Since electrogeneration of the reactive species in the thin solution layer is quantitative, spectral observation of intermediates and products of the chemical reaction is not interfered with by starting material unless a regenerative mechanism is involved. Exhaustive electrolysis of the electroactive species in the thin-layer solution was achieved, and spectra are presented as a function of both electrode potential and time (Figure 3). The finite thickness of the electrode cavity combined with diffusion being the only mode of mass transport resulted in a finite time for complete electrolysis of the solution in the electrocavity, hence the time-dependent spectra shown in Figure 3. The spectra were recorded in multiple potential steps in increments of 100 mV. At potentials more positive than −0.5 V, the absorbance spectrum is similar to that observed in Figure 1, with an intense absorption band at 466 nm and less intense bands at 421, 400, and 379 nm. At −0.5 V, a change in the absorbance spectrum was observed, characterized by the appearance of a new band at 432 nm and the subsequent reduction in intensity of the bands at 379 and 400 nm. The weak band that was observed at 421 nm at potentials more positive than −0.5 V is no longer evident. As bulk electrolysis of the solution is allowed to proceed at −0.5 V, the intensity of the 432 nm band increases while that of the band at 466 nm decreases until the spectrum becomes dominated by the 432 nm band (Figure 3c). MnTSPP was also reduced chemically using sodium dithionite, and the UV−vis absorption spectrum of the reduced porphyrin was obtained. The UV−vis absorbance spectrum of the chemically reduced manganese porphyrin was similar to that of the electrochemically reduced porphyrin.

UV−vis absorbance spectra of a number of reduced Mn porphyrins have been reported in the literature.[36] The absorbance spectrum of Mn^{III} protoporphyrin is characterized by a split Soret band at 465 and 370 nm. When Mn^{III} PP is reduced to the Mn^{II}-PP, a single Soret band at 428 nm is observed. The potential-dependent wavelength shifts of the Soret band in the UV−vis absorbance spectrum of MnTSPP mirror those observed for MnPP.

Electrochemistry. The oxidative and reductive electrochemistry of Mn porphyrins in aqueous medium was studied using polarography and cyclic voltammetry.[37−39] Water-soluble Mn^{III}-TSPP was shown[40] to undergo a well-defined one-electron reduction to the Mn^{II} derivative on a glassy carbon electrode. This reduction has an E_p value of −0.25 V vs NHE at pH 13. Oxidation of Mn^{III} to the corresponding Mn^{IV} species was shown to be fully reversible at pH 13, but became progressively more difficult and less reversible as the pH was decreased.

CV of 10^{-3} M MnTSPP was performed using Pt, Au, and Ag working electrodes. Figure 4 shows the CV of MnTSPP on a silver electrode, while Figure 5 shows DPV of the same solution on a gold working electrode. On all three electrode surfaces, a reductive peak is observed at potentials close to −0.5 V on the cathodic scan. On Pt, this process shows complete reversibility, while on the Au and Ag electrode surfaces the process is irreversible. On both Ag and Au electrode surfaces a second peak at E_p −0.85 V is observed. This peak was absent from the CV on Pt electrode. From the CV data, we concluded that the product of the electrochemical reduction occurring at −0.85 V is strongly adsorbed onto the Ag electrode surface. Reduction of the porphyrin ring produced a strongly adsorbed material that displaces other adsorbed species. Irreversible changes were observed for Mn^{II}HM although extensive studies were unable to characterize these changes.

Examination of the wave at E_p −0.5 V on a Pt electrode indicates a diffusion-controlled process unencumbered by coupled chemical reactions. Plots of i_p vs the square root of scan rate were linear for both peaks on Ag, Au, and Pt electrode surfaces while similiar linearity is observed for the −0.5 V peak on the Pt electrode. Figure 6 shows the plot of peak current vs the square root of scan rate for the peak at −0.85 on a silver electrode surface. A linear relationship is observed with a regression coefficient of 0.99. The linearity between the i_p and

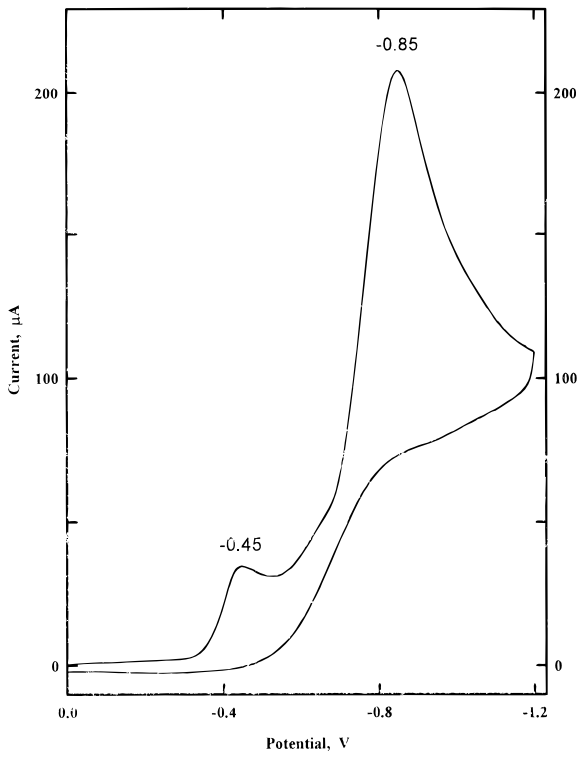

Figure 4. Cyclic voltammetry of MnTSPP on a silver electrode. Potential range from 0.0 V to −1.2 V. Scan rate 300 mV/s, Ag working electrode.

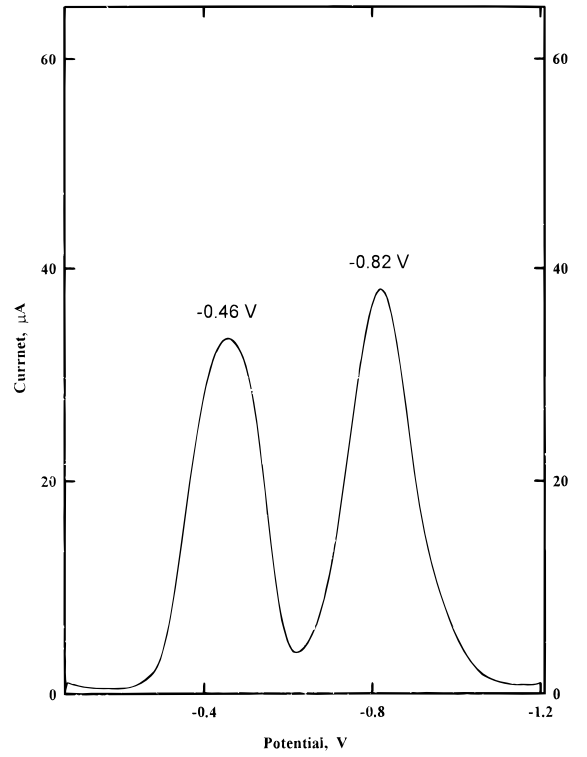

Figure 5. Differential pulse voltammetry of 10^{-3} M MnTSPP on a gold electrode. Potential range from 0.0 to −1.2 V. Scan rate 300 mV/s.

square root of scan rate for the two electrochemical processes indicates that both are Faradaic.

The effect of pH on the E_p of water-soluble metalloporphyrins has been investigated using cyclic voltammetry on a GC electrode.[41] Within the pH range 5−10, no changes were observed for the E_p corresponding to the Mn^{III} to Mn^{II} transition.

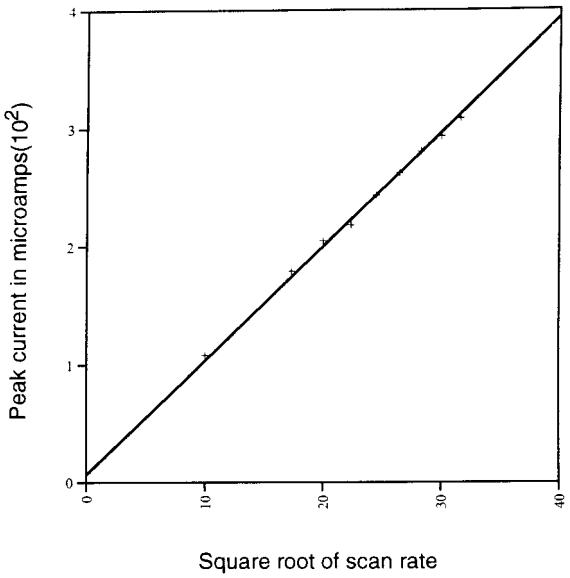

Figure 6. Plot of peak current vs square root of scan rate for the −0.5 V peak.

At pH values more basic than 10, E_p showed a gradual shift to more negative potentials.

Brucie and co-workers[42] investigated the effects of pH on the redox potentials of Fe and MnTPP in aqueous solutions. A significant shift was observed for the half-wave potential for the one-electron reduction of Fe^{III} at a glassy carbon electrode. The value shifted from −0.28 V at pH 3 to −0.59 V at pH 8. Above pH 9.5, the half-wave potential was constant at −0.59 V. Between pH 6 and 8, two reductions were observed, and the measured currents at both high and low pH correspond to a one-electron reduction of Fe^{III}. As the solution pH increased from 6 to 8, the current associated with the reduction at −0.28 V decreased in magnitude and that associated with the reduction at −0.55 V increased.

Shifts in half-wave potentials were observed[42] for the one-electron oxidation of Mn^{III}. The half-wave potential shifted from 1.04 V below pH 3 to 0.86 V at pH 10.08. For manganese hematoporphyrin, half-wave potentials varied with pH in the 1−4 and 11−13 range but were invariant at pH values between 4 and 11, suggesting that hydrogen or hydroxide ions are involved in the electrode reaction at high and low pH values but not at intermediate ones. No variation in E_p as a function of solution pH in the range was observed in this study. The reduction giving rise to the wave around −0.5 V on Pt, Au, and Ag is a one-electron reduction of Mn^{III} to Mn^{II}.

Figure 7 shows the SERS spectra of MnTSPP as a function of electrode potential. SERS spectra of MnTSPP have not been previously reported in the literature. As a result, it was necessary to identify the spectra presented in Figure 7 as either SERS spectra, solution Raman spectra, or a combination of solution and SERS spectra. In situ and ex situ ORC were performed, and Raman spectra were obtained from both surfaces. For the in situ roughening, the ORC was performed in a solution containing MnTSPP, and the electrochemical cell was washed with electrolyte blank before recording of the SERS spectra. For ex situ roughening, the ORC was performed in an electrolyte blank, and the resulting roughened electrode was placed in a dilute solution of the porphyrin. The Raman spectra were then obtained.

Both roughening procedures gave good quality spectra, although the signal intensities from the in situ roughened electrode were much higher than those from the ex situ

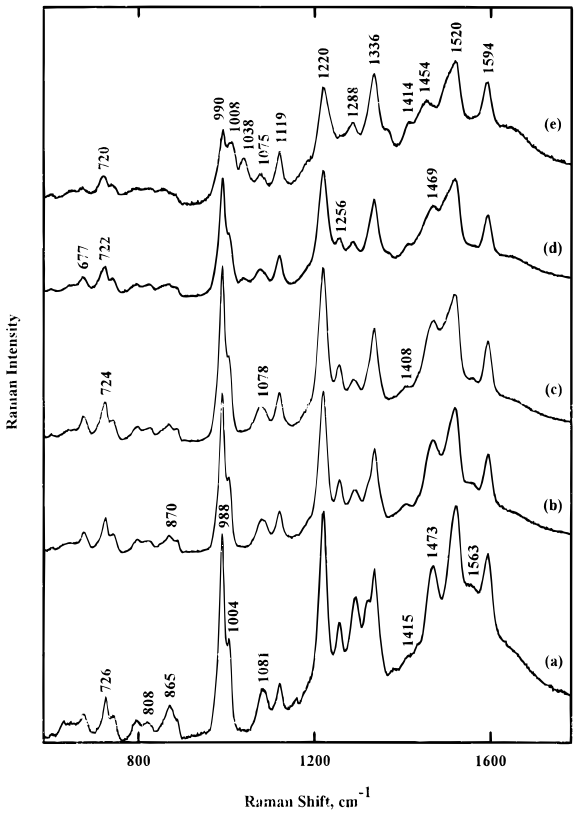

Figure 7. Potential-dependent SERS spectra of MnTSPP on a silver electrode with 488 nm laser excitation.

roughened electrode. In the absence of an anodization process, only a very weak Raman signal was obtained from the silver electrode surface. Polarization measurements were also performed, and polarization ratios close to 0.5 or greater were observed for the spectra obtained after anodization of the electrode surface. The dependence of the intensity of the Raman signal on anodization of the metal surface along with the polarization ratios of the bands and the large signal enhancement of the anodized spectra over the solution bands identify the spectra in Figure 7 as SERS spectra.

Sarkar and Verma[43] have reported resonance Raman spectra of solid and solution tetraphenylporphinato manganese(III) chloride (MnTPP) with 441.6 nm laser excitation and nonresonance-enhanced Raman spectra with excitation at 476.5, 584, and 619.8 nm. The band frequencies of solution Raman spectrum of MnTSPP shown in Figure 8 exhibit excellent agreement with the work of Sarkar.[43] Two spectral regions do however show some differences. Sarkar[43] observed a band at 1486 cm^{-1} which was absent in the solution Raman spectra of MnTSPP. Small differences were also observed in the 900−1030 cm^{-1} region of the spectrum. Raman spectra of MnTPPCl in KBr with 441.6 nm excitation showed two intense bands at 1007 and 997 cm^{-1} along with a shoulder at 1024 cm^{-1}. When excitation was shifted to 530.9 nm, the relative intensities of the bands changed, with the 1007 and 1024 cm^{-1} bands exhibiting moderate intensity and the 997 cm^{-1} appearing as a weak band. The relative intensities of the bands in this region of the spectrum are extremely dependent on excitation wavelength. Resonance Raman spectra of MnTSPP adsorbed on modified resins have also been reported.[44] In these spectra an intense band was observed at 1006 cm^{-1} for the Mn^{III} species, and upon oxidation of the porphyrin, this band shifted to 993 cm^{-1}. No other bands were observed in this region of the spectrum. In the solution Raman spectrum of MnTSPP, Figure

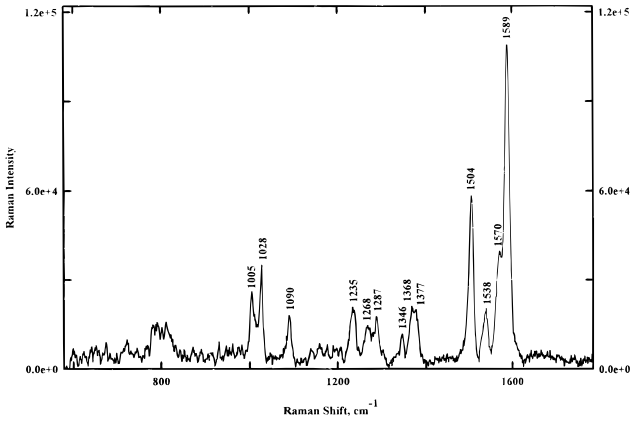

Figure 8. Solution Raman spectrum of 10^{-4} M MnTSPP with 488 nm laser excitation.

8, an intense band is observed at 1028 cm^{-1} while another band is observed at 1005 cm^{-1}. These frequencies are in close agreement with the bands observed by Sarkar at 1024 and 997 cm^{-1}, respectively. The 997 cm^{-1} band, which was observed in the spectra of MnTPP, is not observed in the solution spectra. Potential-dependent changes in the relative intensities of these bands have also been observed in the SERS spectra; these changes will be discussed in a later section.

Resonance Raman spectra were also obtained of MnTPP embedded in the ionic pockets of polymeric Nafion.[45] As was observed for MnTPP, a band was observed at 1453 cm^{-1} in the RR spectra of Mn^{III}TPP embedded in Nafion. This band was absent in our solution Raman spectra; however, excellent agreement was observed between our solution Raman spectrum of MnTSPP and the RR spectra of MnTPP embedded in polymeric Nafion, except that the 1570 cm^{-1} solution Raman band is shifted up to 1579 cm^{-1} in the latter and an upshift of 8 cm^{-1} is observed for the 1589 cm^{-1} band in the former.

Solution Raman Band Assignments. All water-soluble metalloporphyrins exhibit resonance Raman bands of medium to very high intensity in the spectral region above 1000 cm^{-1}. These bands exhibit very little dependence on the porphyrin meso substituents and are due to vibrations of the tetrapyrrole system.[46]

The Raman band assignments, which are proposed in this study, are based on frequency patterns and comparison with published[44,47−50] data. ν_4 has been shown to be an important indicator of the oxidation state of the central metal in the porphyrin macrocycle.[47] Research reveals its sensitivity to the electron withdrawal ability of ligands bound to the central metal.[48] The vibration is usually found in the 1360−1375 cm^{-1} region of the Raman spectrum of Mn porphyrins and has been observed at 1363 cm^{-1} in the resonance Raman spectrum of Mn^{III}TPPCl and at 1370 cm^{-1} for AcMn^{III}PPDME.[49] Two moderately intense bands at 1368 and 1377 cm^{-1} were observed in our solution Raman spectrum of MnTSPP and were assigned to the ν_4 and ν_{29} vibrations, respectively, based on frequency patterns.

The ν_3 vibration, which possesses a large $C_\beta-C_\beta$ component, was observed at 1470 cm^{-1} in NiTPP[50] and 1456 cm^{-1} in Mn^{III}-TPP.[44] This vibration is also observed at frequencies of 1500 and 1494 cm^{-1} for AcMn^{III}PPDME and Py$_2$Mn^{III}PP,[49] respectively, and its frequency is highly dependent on the coordination state of the central metal. The high value of ν_3 in this study, 1504 cm^{-1}, is suggestive of a six-coordinated Mn porphyrin. A similar result, 1498 cm^{-1}, was obtained for manganese-substituted myoglobin and hemoglobin.[49]

TABLE 1: Vibrational Assignments of Normal Raman and SERS Spectral Frequencies for MnTSPP with a 488 nm Excitation

Raman	SERS	vibrational assignments of MnTSPP	modes[b]	Spiro[c]
1589 s[a]	1594 s	ν_{10}, $\nu(C_\alpha C_m)$ (87) + $\delta(C_\alpha C_{Ph})$ (7)	2	1594
1570 m	1563 w	ν_2, $\nu(C_\alpha C_m)$ (29) + $\nu(C_\beta C_\beta)$ (15) + $\nu(CC)_{Ph}$ (18)	1	1572
		ν_{19}, $\nu(C_\alpha C_m)$ (100) + $\nu(C_\alpha C_m C_{Ph})$	3	1550
1538 m	1520 s	ν_{38}, $\nu(C_\beta C_\beta)$ (67) + $\delta(C_\beta H)$ (26)	2	1504
1504 s	1473 s	ν_3, $\nu(C_\beta C_\beta)$ (44) + $\nu(C_\alpha C_m)$ (19) + $\delta(CCH)_{Ph}$ (11)	2	1470
1377 m	1415 w	ν_{29}, $\nu(C_\alpha C_\beta)$ (43) + $\delta(C_\beta H)$ (48) + $\delta(C_\alpha C_\beta)$ (10)	4	1377
1368 m	1336 s	ν_4, $\nu(C_\alpha C_\beta)$ (42) + $\nu(NC_\alpha)$ (21) + $\delta(C_\alpha NC_\alpha)$ (18) + $\delta(C_\alpha C_m)$ (18)	1	1374
1287 m	1288 w	ν_{27}, $\nu(C_m Ph)$ (31) + $\nu(NC_\alpha)$ (40) + $\delta(CH)_{Ph}$ (13)	4	1269
1235 m	1220 s	ν_1, $\delta(C_m Ph)$ (37) + $\nu(NC_\alpha)$ (19) + $\nu(CC)_{Ph}$ (12) + $\delta(CCH)_{Ph}$ (21)	1	1235
1090 m	1081 m	ν_9, $\delta(C_\beta H)$ (64) + $\nu(C_\beta C_\beta)$ (10)	1	1079
1028 m		ν_{22}, $\nu(C_\alpha C_\beta)$ (38) + $\nu(NC_\alpha)$ (23) + $\delta(C_\beta H)$ (22)	3	1016
1005 m	988 s	ν_6, $\nu(C_\alpha C_\beta)$ (27) + $\nu(NC_\alpha)$ (93) + $\nu(CC)_{Ph}$ (22)	1	1004

[a] Intensities: w = weak, m = medium, s = strong. [b] Modes: 1 = A_{1g} skeletal mode, 2 = B_{1g} skeletal mode, 3 = A_{2g} skeletal mode, 4 = B_{2g} skeletal mode, 5 = phenyl in-plane mode, 6 = phenyl out-of-plane mode. [c] Li, Czernuszewicz, Kincaid, Su, and Spiro, *J. Phys. Chem.* **1990**, *94*, 31−47.

TABLE 2: List of Core Size Frequencies for Mn^{III}TSPP

band	freq, cm^{-1}	band	freq, cm^{-1}
ν_{10}	1589	ν_3	1504
ν_2, ν_{19}	1570	ν_4	1368
ν_{11}	1538		

There is some ambiguity over the assignment of the ν_2 and ν_{10} vibrational modes. In resonance Raman spectra of NiTPP,[50] the 1594 cm^{-1} band is assigned to the ν_{10} vibration and the 1572 cm^{-1} band to the ν_2 vibration. ν_2 was been assigned to the 1580 cm^{-1} band in five-coordinate $AcMn^{III}$PPDME and 1573 cm^{-1} for the six-coordinate py_2Mn^{III} PP, while ν_{10} is at 1634 cm^{-1} for the five-coordinate species and 1627 cm^{-1} for the six-coordinate species.[49] Maclean et al.[44] have assigned the 1579 and 1556 cm^{-1} bands to the ν_{10} and ν_2 vibrations, respectively, for MnTPP dissolved in DMF and embedded in Nafion. The vibrations at 1589 and 1570 cm^{-1} were therefore tentatively assigned to ν_{10} and ν_2, respectively.

The 1377 cm^{-1} band observed in our solution Raman spectrum of MnTSPP exhibits a frequency similar to the 1377 cm^{-1} band found in the resonance Raman spectrum of NiTPP[50] and is, therefore, assigned to the $\nu(C_\alpha-C_\beta) - \delta(C_\beta-H)$ ν_{29} vibration.

A comparison of the solution Raman spectra of MnTSPP with 488 nm excitation and $AcMn^{III}$PPDME[49] revealed excellent agreement in the frequencies of ν_4, ν_3, and ν_2. ν_4 was observed at 1368 cm^{-1} in this study and at 1370 cm^{-1} for the five-coordinate Mn^{II}PPDME compound. ν_3 was at 1503 cm^{-1} for Mn^{III}TSPP and 1500 cm^{-1} for Mn^{III}PPDME while a 8 cm^{-1} shift was observed for ν_2. Calculation of the core size of MnTSPPCl, based on constants developed by Spiro et al., yielded a value of 1.961 compared to a value of 1.990 for Mn^{III}-TPPCl.

The frequencies of ν_2 and ν_{19} bands overlap, being separated by less than 3 cm^{-1}. They were assigned by Spiro,[49] based on the anomalous polarization properties of the A_2g ν_{19}**.** Consequently, the band observed in the solution Raman spectrum at 1570 cm^{-1} was assigned as a combination of the ν_2 and ν_{19} bands, which were unresolvable given the resolving power of the grating used in this study.

The other core-sensitive vibration, ν_{11}, was assigned to the band at 1538 cm^{-1} in our solution spectrum of MnTSPP. Table 1 lists the assignments of the vibrational modes of MnTSPP, while Table 2 lists the core size marker band frequencies for Mn^{III}TSPP.

SERS Band Assignments. SERS spectra of MnTSPP are observed at −0.6 V. Significant differences in the band intensities and frequencies are observed for the SERS spectra at −0.6 V relative to the solution spectrum. The SERS spectrum, Figure 7a at −0.6 V, is dominated by bands at 988, 1220, and 1520 cm^{-1}, while bands of moderate intensity were observed at 1336, 1473, and 1594 cm^{-1}. Less intense bands were observed at 1288, 1256, 1119, and 1081 cm^{-1}. Significant changes in band frequencies were observed between the SERS spectrum at −0.6 V and the solution Raman spectrum. The strong 1589 cm^{-1} band in the solution spectrum was replaced by a moderately intense band at 1594 cm^{-1} in the SERS spectrum. This band was assigned to the ν_{10} vibration, which is upshifted by 5 cm^{-1} relative to the solution values. ν_2 is the weak band at 1563 cm^{-1} in the SERS spectrum, while ν_{38} is the most intense SERS band and is found at 1520 cm^{-1}.

The 1400 cm^{-1} region of the solution Raman spectrum was devoid of Raman bands. In the SERS spectrum, however, two bands were observed in this spectral region. The first is a moderately intense band at 1473 cm^{-1}, and the second is a weak band at 1415 cm^{-1}. The 1473 cm^{-1} band is assigned to the ν_3 vibration, which was found at 1464 cm^{-1} in the Raman spectrum of five-coordinate Mn^{II}PP.[49] A 1418 cm^{-1} band was reported in the Raman spectrum of (2MeImH)Mn^{II}PP, but this band was not reported in the Raman spectrum of (2MeImH)Mn^{II}TPP.[49] The assignment of this band to a $\delta(CH_2)$ vibration in PP cannot be extrapolated to MnTSPP because no such CH_2 group exists in this molecule.

Another striking difference between the solution and SERS spectra is in the frequency of ν_4. This band, which was observed at 1368 cm^{-1} in the solution spectrum, is downshifted by 32 cm^{-1} to 1336 cm^{-1} in the SERS spectrum at −0.6 V. The frequency of ν_4 has been shown to be a sensitive indicator of the oxidation state of the central metal. Shifts in the frequency of this band have been correlated with changes in the oxidation state of the metal. The observed shift is characteristic of a change in the oxidation state of the central Mn atom in the porphyrin system from III in the solution to II at −0.6 V on the silver electrode surface. A similar shift was observed for this band, which is found at 1363 cm^{-1} in the Raman spectrum of Mn^{III}-TPPCl and 1340 cm^{-1} in (2MeImH)Mn^{II}TPP.[49] ν_3 revealed a shift from 1504 cm^{-1} in the solution Raman spectrum to 1473 cm^{-1} in the SERS spectrum. Table 3 compares the core size marker band frequencies of Mn^{II}TSPP with those of Mn^{II}PP.

Along with the skeletal modes, a number of substituent modes were observed in the resonance Raman and SERS spectra of porphyrins. Cotton observed bands at 1597 and 886 cm^{-1} in the SERS spectra of TSPP adsorbed on a silver electrode. These bands were assigned to phenyl mode vibrations. The 1599 cm^{-1} band was also observed in the resonance Raman spectra of tetraphenyl porphyrins. These phenyl modes gained enhance-

TABLE 3: Comparison of Core Size Marker Frequencies (cm^{-1}) for Mn^{II}TSPP and Mn^{II}PP

band	Mn^{II}PP V coordinate	Mn^{II}PP IV coordinate	Mn^{II}TSPP SERS
ν_{10}	1595	1555	1594
ν_{37}	1575	1548	
ν_2	1569	1540	1563
ν_{11}	1536	1506	
ν_{38}	1513	1478	1520
ν_3	1464	1438	1473

ment by mixing with a skeletal mode and borrowing some of its enhancement. No such bands were observed in the SERS spectra of MnTSPP in this study.

Discussion

Porphyrin Aggregation. UV−vis absorption spectroscopy has been extensively used to determine the effect of experimental conditions such as pH and ionic strength on the molecular association of water-soluble porphyrins, particularly the sulfonated tetraphenylporphyrin systems. Under specific experimental conditions, intermolecular attractions can result in dimer formation in a number of metallo TSPP compounds.

The presence of TSPP derivatives adsorbed in the aggregated state on Ag electrodes and sols was used to account for certain electrochemical and spectroscopic properties of these molecules.[51] Two electrochemical processes, monitored by changes in the SERS spectra, have been attributed to the dissociation of the surface-bound aggregated TSPP to the monomer, followed by silver incorporation.[52,53]

SERS spectra of TSPP on silver colloids show bands at 702, 318, and 238 cm^{-1}, which are not observed in the solution spectra and are close in frequency to bands observed at 698, 313, and 240 cm^{-1} for the SERS spectra of TSPP on a silver electrode.[52] These vibrations were explained as due to adsorption of the porphyrin molecule in the aggregated state.

The linearity of the Beer's law plot, along with the absence of bands around 700 and 318 cm^{-1} in the SERS spectra of MnTSPP, indicated that the molecule is adsorbed onto the electrode surface as a monomer and not as a dimer, as has been proposed for other water-soluble metallo and free-base TSPP derivatives. Examination of the SERS spectral region below 720 cm^{-1} failed to identify bands at the frequencies observed by Itoh and Mon et al.,[52] which are characteristic of porphyrin aggregation on the surface.

Porphyrin Orientation. Surface selection rules[55,56] are founded on the electromagnetic theory of SERS intensities. The incident light increases the electromagnetic field at the surface of small metal particles and, thus, amplifies the scattered intensity and the Raman excitation intensity. From this, vibrational modes of adsorbed surface species, which involve changes in the molecular polarizability with a component normal to the surface, would show the greatest enhancement. For Raman spectroscopy the normal mode of out-of-plane vibrations results in a change in the dipole moment component perpendicular to the molecular plane. For in-plane vibrations this change in dipole moment is parallel to the plane of the molecule.

The relative Raman intensities of the porphyrin ring vibrations, at 1600 and 808 cm^{-1}, have served as sensitive indicators of the orientation of the adsorbed porphyrin molecules.[57]

Previous studies of TPP and its phenyl-substituted analogues have demonstrated that the porphyrin is adsorbed with its molecular axis parallel to the electrode surface, thereby bonding to the surface through its π-electron system. In the SERS spectrum at −0.5 V no band is observed at 1600 cm^{-1} while a moderately intense band appears at 808 cm^{-1}. This is similar to what was observed for TSPP adsorbed on HNO_3-roughened silver foils. In both instances the porphyrin molecule is adsorbed with its molecular axis parallel to the electrode surface.

Electrochemistry. The electrochemical data indicate two Faradaic reductive processes occurring at −0.5 and −0.9 V on a silver working electrode. Potential-dependent changes in the UV−vis absorbance spectra indicate that at potentials more positive than −0.5 V the porphyrin exists as Mn^{III} (466 nm Soret band) and is reduced to the Mn^{II} species (Soret band at 432 nm), at −0.5 V. Further confirmation of the presence of the Mn^{II} species is obtained from the SERS spectra which show shifts in the ν_4 and ν_3 vibrations, the frequencies of which are now characteristic of the Mn metal in the II redox state.

The Mn^{III} to Mn^{II} reduction in porphyrins was performed chemically in aqueous and organic solvents as well as electrochemically in CH_2Cl_2 and spontaneously in the vapor phase.[58] Rate constants for the dithionite reduction of MnTSPP at pH 7.5 have resulted in $K_0/s^{-1} = 16$ and $K_A/10^6$ dm^3 mol^{-1} s^{-1} of 6.4, with reduction being first order in concentration.

Coordination State. Carnierer et al.[59] have proposed coordination states for Mn^{III}TSPP in aqueous solution. In the pH range 5−11 two p*K* transitions were proposed for Mn^{III}TSPP. In all three species, $Mn^{III}(OH_2)_2$, $Mn^{III}(OH)(OH_2)$, and $Mn^{III}(OH)_2$, the Mn^{III} is six-coordinated. The coordination ligands are two water molecules in the acidic region and two hydroxide ligands at the basic end of the spectrum. The intermediate species is also six-coordinate with a water molecule and a hydroxide ion serving as the ligands. Between pH 3 and 11 $Mn^{III}(OH_2)_2$ undergoes a one-electron reduction to $Mn^{II}(OH_2)$ or $Mn^{III}(OH)(OH_2)$ undergoes a one-electron reduction to form $Mn^{II}(OH_2)$. At pH values above 11, $Mn^{III}(OH)_2$ undergoes a one-electron reduction to form either $Mn^{II}(OH)$ or $Mn^{II}(OH_2)$. All the proposed schemes start with a six-coordinate Mn^{III} porphyrin which undergoes a one-electron reduction to form the five-coordinate Mn^{II} species.

It is well established[60] that the Raman spectra of porphyrins and heme proteins contain bands that are sensitive to the spin state, coordination number, and oxidation state of the central metal. Spaulding et al.[61,62] have established a consistent correlation between ν_{19} and the core size of the porphyrin cavity. This core size marker band is sensitive to the spin state, primarily because the size of the central atom is dependent on the spin state. Relatively small differences in the core size (−0.06 Å) can result in Raman shifts of 5−6 cm^{-1}. The spin state marker bands in resonance Raman and SERS spectra of metalloporphyrins tend to be found in the high-frequency region of the spectrum between 1350 and 1700 cm^{-1}. ν_2 and ν_3, which are A_{1g} modes, ν_{10} and ν_{11}, which are B_{1g} and B_{2g} modes, and ν_{19}, which is an A_{2g} mode, have been shown to be core size sensitive.

Table 3 compares the core size marker frequencies of Mn^{II}TSPP with those for four- and five-coordinate Mn^{II}PP. The five-coordinate porphyrin spectra are characterized by an upshift in the frequencies of ν_{10}, ν_2, ν_{38}, and ν_3 relative to their frequencies in the four-coordinate state. The excellent agreement between the spectra of Mn^{II}TSPP and that of the five-coordinate Mn^{II}PP allows for the conclusion that Mn^{II}TSPP is five-coordinate when adsorbed onto the silver electrode surface. The nature of the fifth ligand, OH_2 or OH, cannot be determined from the SERS data.

Porphyrin Radical Anions. The spectrum in Figure 7e represents the SERS spectrum of the Mn^{II}TSPP radical anion. Resonance Raman spectra and normal-coordinate calculations

have been performed on reduced $Zn^{II}TPP$ anion and a number of its isotopically substituted analogues. These calculations suggest that the reduction of the porphyrin macrocycle results in a change in composition of the eigenvectors of certain $C_\alpha-C_\beta$ vibrations but not others, particularly $C_\alpha-C_m$ modes at 1549 and 1514 cm^{-1} in the spectrum of $ZnTPP^-$.

Changes in the eigenvectors, on reduction of the porphyrin macrocycle, are due to b_{1g}-like Jahn−Teller distortion to D_{2h} symmetry. Interpretation of the vibrational spectrum of the anion should therefore be performed in terms of D_{2h} symmetry, not the symmetry of the parent complex.

Conclusions

The results presented in this study demonstrate the applicability of SERS in determining the reduction products of the water-soluble MnTSPP at a silver electrode. The aggregation state and orientation of the adsorbed porphyrin are determined from absorbance spectroscopy and SERS. Potential-dependent UV−vis absorption spectroscopy and SERS spectra confirm that the process observed at −0.5 V on the silver electrode involves the metal-centered reduction of the Mn from the III to the II oxidation state. Band assignments are presented for the solution Raman and SERS spectra of MnTSPP. The frequencies of the core size marker bands in the solution Raman spectrum of Mn^{III} TSPP indicate that the Mn is six-coordinate while the SERS spectrum of Mn^{II} indicates that on reduction the coordination state of the central metal changes to five-coordinate. This study further demonstrates the utility of SERS as an analytical technique capable of providing detailed information regarding adsorbate/surface interaction.

Acknowledgment. This work was supported by the National Institutes of Health MBRS/NIGMS, Grant S06GM08016. P.H. is indebted to NASA under Grant NCC-5-185.

References and Notes

(1) Spiro, T. G.; Czernuszewicz, R. S.; Li, X. Y. *Coord. Chem. Rev.* **1990**, *100*, 541.
(2) Kitagawa, T.; Mizutani, Y. *Coord. Chem. Rev.* **1994**, *135/136*, 685.
(3) Tu, A. T. *Raman Spectroscopy in Biology: Principles and Applications;* John Wiley and Sons: New York, 1982; Chapter 12.
(4) Longo, F. R. *Advances in Porphyrin Chemistry*; Ann Arbor Science Publishers: Ann Arbor, MI, 1979.
(5) Chumanov, G.; Picorel, R.; Toon, S.; Siebert, M.; Cotton, T. M. *Photochem. Photobiol.* **1993**, *58*, 757.
(6) Carnier, N.; Harriman, A.; Porter, G. *J. Chem. Soc., Dalton. Trans.* **1982**, 931.
(7) Gallion, L.; Bedioui, F.; Battioni, P.; Devynck, J. *J. Mol. Catal.* **1993**, *78*, L23.
(8) Bedioui, F.; Gutierrez-Granados, S.; Devynck, J.; Bied-Charreton, C. *New J. Chem.* **1991**, *15*, 939.
(9) Arasasinghan, R. D.; Bruice, T. C. *Inorg. Chem.* **1990**, *29*, 1422.
(10) Bettelheim, A.; Ozer, D.; Weinraub, D. *J. Chem. Soc., Dalton Trans.* 1**986**, 2297.
(11) Gutierrez-Granados, S.; Bedioui, F.; Devynck, J. *Electrochim. Acta* **1991**, *38*, 1747.
(12) Nishihara, H.; Pressprich, K.; Murray, R. W.; Collman, J. P. *Inorg. Chem.* **1990**, *29*, 1000.
(13) Hosten, C. M.; Birke, R. L.; Lombardi, J. R. *J. Phys. Chem.* **1992**, *96*, 6585.
(14) Nabiev, I. R.; Chumanova, G. D.; Manykin, E. A. *Sov. Phys. J.* **1985**, *28*, 204.
(15) Feofanov, A.; Janoul, A.; Oleinika, V.; Gromov, S.; Fedorova, O.; Alfimov, M.; Nabiev, I. *J. Phys. Chem.* **1996**, *100*, 2154.
(16) Tolia, A. A.; Williams, C. T.; Takoudis, C. G.; Meaver, M. J. *J. Phys. Chem.* **1995**, *99*, 4599.
(17) Feilchenfeld, H.; Chumanov, G.; Cotton, T. M. *J. Phys. Chem.* **1996**, *100*, 4937.
(18) Koyams, T.; Yamaga, M.; Kim, M.; Itoh, K. *Inorg. Chem.* **1985**, *24*, 4258.
(19) Lu, T.; Cotton, T. M.; Hurst, J. K.; Thompson, D. H. P. *J. Phys. Chem.* **1988**, *92*, 6978.
(20) Rubin, J. C.; Cocio, P.; Ribeiro, M.; Matz, M. *J. Phys. Chem.* **1995**, *99*, 15765.
(21) Sanchez, L. A.; Spiro, T. G. *J. Phys. Chem.* **1985**, *89*, 7368.
(22) Cermakova, K.; Vlckova, B.; Fort, V.; Lednicky, F. *J. Mol. Struct.* **1995**, *349*, 129.
(23) Matejka, P.; Mojzes, P.; Vlckova, B. *J. Mol. Struct.* **1995**, *349*, 121.
(24) Vlckova, B.; Matejka, P.; Simonova, J.; Cermakova, K.; Pancoska, P.; Baumruk, V. *J. Phys. Chem.* **1993**, *97*, 9719.
(25) Tai, Z.; Zhang, J.; Gao, J.; Xue, G. *J. Mater. Chem.* **1993**, *3*, 417.
(26) (a) Mou, C.; Chen, D.; Wang, X.; Zhang, B.; He, T.; Xin, H.; Liu, F. *Spectrochim. Acta* **1991,** *47A*, 1575. (b) Vlckova, B.; Matejka, P.; Pancoska, P.; Baumruk, V.; Kral, V. *Inorg. Chem.* **1991**, *30*, 4103.
(27) Mou, C.; Chen, D.; Wang, X.; Zhang, B.; He, T.; Xin, H.; Liu, F. *Chem. Phys. Lett.* **1991**, *179*, 237.
(28) Song, O. K.; Yoon, M. J.; Kim, D. *J. Raman Spectrosc.* **1989**, *20*, 739.
(29) Matejka, P.; Vlckova, B.; Vohlidal, J.; Pancoska, P.; Baumruk, V. *J. Phys. Chem.* **1992**, *96*, 1361.
(30) Song, O. K.; Shin, E.; Lee, M.; Kim, D.; Han, J. T.; Jee, J. G.; Yoon, M. *J. Raman Spectrosc.* **1992**, *23*, 667.
(31) Shi, C.; Zhang, W.; Birke, R. L.; Gosser, D. K.; Lombardi, J. R. *J. Phys. Chem.* **1991**, *95*, 6276.
(32) Shi, C.; Zhang, W.; Birke, R. L.; Lombardi, J. R. *J. Phys. Chem.* **1992**, *96*, 10093.
(33) Edwards, L.; Dolphin, D. H.; Goutterman, M. *J. Mol. Spectrosc.* **1970**, *35*, 90.
(34) Asher, S.; Sauer, K. *J. Chem. Phys.* **1976**, *64*, 4115.
(35) Goutterman, M. In *The Porphyrins;* Dolphin, D., Ed.; Academic Press: New York, 1978; Vol. III, p 347.
(36) Harriman, A.; Porter, G. *J. Chem. Soc., Faraday Trans. 2* **1979**, *75*, 1532.
(37) Hambright, P.; Williams, R. F. X. In *Porphyrin Chemistry Advances*; Longo, F. R., Ed.; Ann Arbor Science: Ann Arbor, MI, 1979; p 284.
(38) Bettelheim, A.; Ozer, D.; Parash, R. *J. Chem. Soc., Faraday Trans. 1* **1983**, 1555.
(39) Kalyanasundaram, K.; Neumann-Spallart, M. *J. Phys. Chem.* **1982**, *86*, 5136.
(40) Harriman, A. *J. Chem. Soc., Dalton Trans.* **1984,** 141.
(41) Carnieri, N.; Harriman, A.; Porter, G. *J. Chem. Soc., Dalton Trans.* **1982**, 931.
(42) Kaaret, T. W.; Zhang, G.-H.; Bruice, T. C. *J. Am. Chem. Soc.* **1991**, *113*, 4653.
(43) Sarkar, M.; Verma, A. L. *Proc.: Chem. Sci.* **1987**, *99*, 167.
(44) Maclean, A. L.; Armstrong, R. S.; Kennedy, B. J. *J. Raman Spectrosc.* **1995**, *26*, 981.
(45) Odo, J.; Mifune, M.; Iwado, T.; Karasudani, T.; Hashimoto, H.; Motohashi, N.; Tanaka, Y.; Saito, Y. *Anal. Sci.* **1991**, *7*, 555.
(46) Spiro, T. G.; Li, X.-Y. In *Biological Applications of Raman Spectroscopy*; Spiro, T. G., Ed.; Wiley-Interscience: New York, 1988; Vol. II, Chapter 1.
(47) Spiro, T. G.; Burke, J. M. *J. Am. Chem. Soc.* **1976**, *98*, 5482.
(48) Spiro, T. G. *Adv. Protein Chem.* **1985**, *37*, 111.
(49) Parthasarathi, N.; Spiro, T. G. *Inorg. Chem.* **1987**, *26*, 3792.
(50) Li, X.-Y.; Czernuszewicz, R. S.; Kincaid, J. R.; Su, Y. O.; Spiro, T. G. *J. Phys. Chem.* **1990**, *94*, 31.
(51) Akins, D. L.; Zhu, H.-R.; Guo, C. *J. Phys. Chem.* **1994**, *98*, 3612.
(52) Itabashi, M.; Kato, K.; Itoh, K. *Chem. Phys. Lett.* **1983**, *97*, 528.
(53) Kim, M.; Tsujino, T.; Itoh, K. *Chem. Phys. Lett.* **1986**, *125*, 364.
(54) Mou, C.; Chen, D.; Wang, X.; Zhang, B.; He, T.; Xin, H.; Liu, F. *Spectrochim. Acta* **1991**, *47A*, 1575.
(55) Creighton, J. A. *Spectroscopy of Surfaces*; John Wiley & Sons: New York, 1988; Chapter 2.
(56) Bandy, B. J.; Llyod, D. R.; Richardson, N. V. *Surf. Sci.* **1979**, *89*, 344.
(57) Tai, Z.; Zhang, J.; Gao, J.; Xue, G. *J. Mater. Chem.* **1993**, *3*, 417.
(58) Davis, D. G.; Montalvo, J. G. *Anal. Chem.* **1969**, *41*, 1195.
(59) Carnieri, N.; Harriman, A.; Porter, G. *J. Chem. Soc., Dalton Trans.* **1982**, 931.
(60) Tu, A. T. *Raman Spectroscopy in Biology: Principles and Applications*; J. Wiley and Sons: New York, p 315.
(61) Spaulding, L. D.; Chang, C. C.; Yu, N.-T.; Felton, R. H. *J. Am. Chem. Soc.* **1975**, *97*, 2517.
(62) Sparks, L. D.; Anderson, K. K.; Medford, C. J.; Smith, K. M.; Shelnutt, J. A. *Inorg. Chem.* **1994**, *33*, 2297.